JPP Journal of Pharmacy and Pharmacology

JPP 2006, 58: 1327–1336

Received April 11, 2006
Accepted June 26, 2006
DOI 10.1211/jpp.58.10.0005
ISSN 0022-3573

Histological evaluation of buccal penetration enhancement properties of chitosan and trimethyl chitosan

G. Sandri, P. Poggi, M. C. Bonferoni, S. Rossi, F. Ferrari and C. Caramella

Abstract

The aim of the present work was to compare the penetration enhancement properties of chitosan hydrochloride (HCS) both as a polymeric solution and as a nanoparticulate system with that of trimethyl chitosan hydrochloride (TMC) on buccal mucosa. The hydrophilic high molecular weight fluorescein isothiocyanate dextran (FD4; 4400 Da) was used as a macromolecule model. The mechanism involved in the HCS (solution and nanoparticles) and TMC solution penetration enhancement was investigated on pig buccal mucosa, characterized by having stratified epithelium and lacking in tight junctions. The permeation/penetration of FD4 and the change in morphology and histology of the mucosa after contact with the polymers were assessed: the experiments were performed ex-vivo by applying the formulations on excised porcine buccal tissue. For the morphology and the histology studies, the epithelial cell layers from freshly excised pig buccal mucosa were analysed with light microscopy by means of routine histopathology analysis (haematoxylin and eosin staining and Toluidine blue staining) and immunohistochemistry reactions. The organization of desmosomal junctions was assessed by means of an immunochemical reaction on desmosomes and transmission electron microscopy. Confocal laser scanning microscopy (CLSM) was used to find evidence of the location of FD4 in the tissue. Furthermore, the increase of the FD4 apparent permeability coefficient was quantified by means of Franz diffusion cells using isolated buccal epithelium to demonstrate the penetration enhancement properties of the polymer systems. Morphological analysis, performed by light microscopy, transmission electron microscopy and CLSM, suggests a similar mechanism of penetration enhancement for both HCS and TMC solutions and for HCS nanoparticles. Such a mechanism probably involves a repackaging of the epithelial cells up to the basal membrane and a partial disarrangement of desmosomes. The cell viability and the nuclear integrity indicated on the semi-thin section stained with Toluidine blue and by CLSM analysis, respectively, suggest that HCS as a polymer solution and a nanoparticulate system, and TMC polymer solution, do not cause cell damage. Trimethyl chitosan and chitosan nanoparticulate systems were able to increase FD4 permeation across buccal epithelium to a greater extent than the chitosan solution.

Department of Pharmaceutical Chemistry, School of Pharmacy, University of Pavia, Pavia, Italy

G. Sandri, M. C. Bonferoni, S. Rossi, F. Ferrari, C. Caramella

Department of Experimental Medicine, Section of Normal Anatomy, University of Pavia, Pavia, Italy

P. Poggi

Correspondence: Carla Caramella, Department of Pharmaceutical Chemistry, School of Pharmacy, University of Pavia, V.le Taramelli, 12, 27100 Pavia, Italy. E-mail: carla.caramella@unipv.it

Funding: This study was supported by funding from the Italian Ministry of University and Scientific Research (MIUR) (PRIN/COFIN 2005).

Introduction

Oligonucleotides and bioactive peptidic molecules and vaccines are very unstable macromolecules and the parenteral route, although invasive and characterized by poor patient compliance, still remains the most used one. Transmucosal routes (buccal, nasal and vaginal) offer the advantages of being non-invasive and easily accessible. In particular, the buccal route is characterized by a strong epithelium able to support mastication and contact with food and beverages, and a pH that is often very different from the physiological environment (Shojaei 1998; Rossi et al 2005). Moreover, this route of administration improves drug bioavailability by avoiding first-pass metabolism and degradation in the gastrointestinal tract. The permeability barrier together with the small area available to drug absorption still remain the main limitations to protein or peptide delivery via the buccal route (Sayani & Chien 1996). Efforts have been made to improve the poor absorption of macromolecules via this route.

Chitosan and trimethyl chitosan are non-toxic, biocompatible and biodegradable polysaccharides: chitosan is derived by means of a partial deacetylation from naturally

occurring chitin (Paul & Sharma 2000), and trimethyl chitosan is obtained through a partial quaternization trimethylation of the aminic groups of chitosan (Sieval et al 1998; Di Colo et al 2004).

Chitosan and trimethyl chitosan have been shown to be potential penetration enhancers in either monostratified or stratified epithelia. In particular, they are able to enhance drug absorption of hydrophilic high molecular weight molecules through monostratified mucosae endowed with tight junctions such as intestinal (Artursson et al 1994; Dodane et al 1999; Thanou et al 2000) and nasal (Hamman et al 2002, 2003) mucosae. It has been shown that they can enhance drug permeation across stratified epithelia lacking in tight junctions such as buccal (Senel et al 2000; Rossi et al 2003a; Sandri et al 2004, 2005b) and vaginal (Rossi et al 2003b) mucosae. Finally, chitosans can improve drug absorption through stratified epithelia with tight junctions such as corneal epithelium (Yi et al 2000; Reichl & Muller-Goymann 2003; Di Colo et al 2004).

In epithelia rich in tight junctions, penetration enhancement by chitosan and trimethyl chitosan is mainly due to a transient widening of the junctions between cells (Kotzè et al 1998; Dodane et al 1999). The mechanism of penetration enhancement across stratified epithelia that lack tight junctions has yet to be completely clarified (Kotzè et al 1998; Senel et al 2000; Senel & Hincal 2001).

Chitosan nanoparticles have been referred to as capable of being absorbed into mucosal tissue (Ma & Lim 2003) and have been found in the cytoplasm, while chitosan macromolecules have been located in the extracellular spaces. The nanoparticle absorption mechanism is probably endocytosis (physiological mechanisms of uptake of membrane proteins and lipids, extracellular ligands and soluble molecules from the cell surface) either by means of clathrin-dependent or clathrin-independent pathways as a function of the interaction with the cellular membranes (Behrens et al 2002; Ma & Lim 2003).

The aim of the present work was to investigate the mechanisms involved in the enhancement of buccal permeation by chitosan hydrochloride (HCS), used both as a polymer solution and as a nanoparticulate system, and by trimethyl chitosan hydrochloride (TMC). As a macromolecule model, fluorescein isothiocyanate dextran (FD4) was used, as it is a hydrophilic high molecular weight molecule (4400 Da) with molecular weight similar to those of some peptidic drugs such as insulin (5788 Da). The HCS (solution and nanoparticles) and TMC penetration enhancement mechanism in pig buccal mucosa, a stratified epithelium lacking in tight junctions, was studied by assessing the permeation of FD4 and the morphology of the mucosa after exposure to the considered polymers.

The morphology of pig buccal mucosa, before and after contact with the polymer systems, was assessed by means of light microscopy using routine histology analysis (sections stained with haematoxylin and eosin and semi-thin sections stained with Toluidine blue). Furthermore, to demonstrate the state of desmosomal junctions after the polymer treatment, an immunohistochemical reaction on desmosomes was performed on semi-thin sections and, in addition, ultra-thin sections were analysed by means of transmission electron microscopy (TEM). The tissue slices were also analysed using confocal laser scanning microscopy (CLSM) to determine the location of FD4 in the tissue. The FD4 apparent permeability coefficient (P_{app}) values after polymeric system treatment were evaluated using heat-isolated buccal epithelium by means of Franz diffusion cells.

Materials and Methods

Materials

TMC (degree of quaternization 46%) was obtained from chitosan (90% deacetylated) with a molecular weight of 580 kDa derived from shrimp (HCS) (ChitoClear FG90; Primex, Haugesund, Norway) using procedures described in literature (Sieval et al 1998). The polymers were previously characterized by Di Colo et al (2004).

Pentasodium tripolyposphate (TPP) (Sigma, Milan, Italy) was used as a chitosan cross-linking agent.

FD4 (Sigma) was used as a model hydrophilic, high molecular weight molecule (4400 Da).

Sample preparation

HCS and TMC were hydrated in distilled water at 4% (w/w) under gentle stirring at room temperature and FD4 was added at 0.2% (w/w).

HCS nanoparticles were prepared according to the mild operation procedure previously developed by Calvo et al (1997) based on ionotropic gelation of chitosan polycation with TPP polyanion. The ionotropic gelation takes place when the positively charged amino groups of chitosan interact with the negatively charged TPP. Chitosan was dissolved at 2.5 mg mL^{-1} in distilled water by means of gentle stirring. TPP was dissolved at 1.25 mg mL^{-1} in distilled water and FD4 was added at 0.2% (w/v). The optimal weight ratio between polymer and TPP was evaluated by turbidimetric analysis as previously described (Sandri et al 2005a). A fixed amount of TPP solution was added by drops to 3 mL of HCS solution and the mixture was diluted to 4.5 mL. The final concentrations were 1.67 mg mL^{-1} for HCS and 0.28 mg mL^{-1} for TPP. The nanoparticles were spontaneously formed by the incorporation of TPP to the polymer solution under vigorous stirring. The FD4-loaded nanoparticles were prepared using the same procedure: FD4 was dissolved at 10 mg mL^{-1} in TPP solution to give, in the polymer–TPP mixture, a final concentration of 0.33 mg mL^{-1}. The nanoparticle colloidal dispersion was used as such in the permeation experiments. The nanoparticle diameter was evaluated by photon correlation spectroscopy (N5 nanosizer; Beckmann Coulter, Milan, Italy) and was 232.8 nm (s.d. = 13.1) with a polydispersity index of 0.486 (s.d. = 0.06).

Morphological and ultrastructural analysis

The pig cheek was obtained from the local slaughterhouse. The pig buccal mucosa was excised immediately after death, maintained in an oxygenated Krebs buffer and used within 1 h. The muscular layer was removed and the epithelium together with the fully maintained connective tissue was used

for the experiment. The buccal epithelium with connective tissue was placed between the donor and acceptor chamber of a flow-through Franz cell. During the experiment, the receptor phase (Krebs buffer) was continuously injected with oxygen. Then, 100 mg of the HCS and TMC polymer solutions and the HCS nanoparticle suspension were spread over the buccal mucosa. Phosphate buffer at pH 6.4 (2 mL) (USP 29) was added over the polymeric sample. The same experiment was performed without polymer (control). The exposure time was 1 h.

At the end of the experiment, the buccal mucosa tissue samples were rinsed twice in Krebs buffer, cut into small portions and each portion processed for morphological evaluation.

Light microscopy analysis

Using a light microscope (Leitz Orthoplan, Milan, Italy), light microscopy analysis was performed on three portions of each tissue processed using three different techniques: haematoxylin and eosin, Toluidine blue and immunohistochemical staining. The microscopic field of vision was photographed using a digital camera (PowerShot; Canon, Tokyo, Japan) and the microphotographs collected by means of Remote Capture and Zoom Browser software (Canon).

Haematoxylin and eosin staining

A portion of each tissue was fixed in buffered 10% formalin and embedded in paraffin wax. Then, 5 μm sections were placed on microscope slides, deparaffinized using xylene, and rehydrated using ethanol solutions in a gradient of 80% up to 100% and distilled water. The tissue slices were placed in 0.7% w/w haematoxylin solution (Sigma), rinsed twice in acid ethanol (0.1 N HCl in 95% ethanol) to remove the excess stain, and left overnight in distilled water. Subsequently, the tissue slices were placed in 0.1% w/w eosin solution (Sigma) and dehydrated using solutions of ethanol in a gradient of 80% up to 100% and then xylene.

Toluidine blue staining

Another portion of each tissue was fixed in 2.5% glutaraldehyde and 1% paraformaldehyde in 0.1 M sodium cacodilate buffer for 3 h at 4°C, post-fixed in 1% osmium tetroxide for 1 h at 4°C, and embedded in an epoxy resin. Semi-thin sections (0.5 μm) were placed on microscope slides, deparaffinized using xylene, and rehydrated using ethanol solutions in a gradient of 80% up to 100% and distilled water. Semi-thin sections (0.5 μm) were stained with a solution of 0.2% w/w (1:400) Toluidine blue (Sigma) in 1% sodium chloride aqueous solution adjusted to pH 2.5 with glacial acetic acid.

Immunohistochemical staining

Pig buccal mucosae that had come into contact with the polymers were embedded in OTC compound and cut perpendicularly to the surface using a cryostat (Leica CM1510; Leica Microsystems, Milan, Italy) at −20°C. Each slice (10 μm thickness) was placed on a microscope slide, dehydrated for 12 h and subsequently fixed by dipping the slides into 30% acetone diluted with phosphate buffered saline (PBS) for 10 min at 4°C. The sections were blocked with 5% fetal calf serum (FCS) diluted in PBS and were incubated overnight at 4°C with the anti-desmosomal protein antibody solution (1:400 in 5% FCS diluted in PBS) (Sigma). Subsequently, they were incubated and reacted with peroxidase conjugated goat anti-mouse IgG antibody (1:200 in 5% of FCS diluted in PBS) (Sigma).

TEM analysis

A further portion of each tissue was blocked in 4% formaldehyde and 1% glutaraldehyde in 0.1 M phosphate buffer at pH 7.4 for at least 2 h or overnight. Subsequently, the portion was washed in 8% (0.2 M) sucrose 0.1 M phosphate buffer at pH 7.4 for three cycles of 5 min each. The portion was post-fixed in 1% osmium tetroxide in 0.1 M phosphate buffer at pH 7.4 for 1 h. The tissue was dehydrated using an ethanol gradient from 50% up to 100%, and subsequently in propylene oxide. The tissue was embedded in an epoxy resin and completely dehydrated in an oven at 60°C for 48 h. Ultra-thin sections (60–90 nm thick) were cut and collected onto grids. The sections were dried overnight before staining. The grids were stained with a solution containing 5% uranyl citrate and lead citrate (0.08 M in lead). The grid was allowed to dry for another 10 min and was then examined using TEM (Zeiss EM109; Zeiss, Milan, Italy).

CLSM analysis

CLSM was used to visualize FD4 in the tissues. Buccal mucosa that had come into contact with polymers was embedded in OTC compound. Slices (10 μm thick) perpendicular to the mucosa surface were cut using a cryostat (Leica CM1510; Leica Microsystems) at −20 °C. Each slice was placed on a microscope slide, dehydrated for 12 h and subsequently fixed by dipping the slides into acetone.

The nuclei of the tissue slices were stained by dipping the biological substrates into a solution (1:100 000) of Hoechst 33258 (Sigma).

Each slide was mounted using polyvinyl alcohol mounting medium with DABCO antifading solution (mixture of tris (hydroxymethyl)amininomethane, tris/hydroxymethyl)aminomethane hydrochloride, polyvinyl alcohol 22 000 Da, glycerol anhydrous and 1,4-diazabicyclo[2.2.2]octane; Bio Chemika, Fluka, Milan, Italy) and covered with a cover glass.

The slides were subjected to CLSM using an excitation wavelength of 488 nm and an emission wavelength of 521 nm for the visualization of FD4, and an excitation wavelength of 346 nm and an emission wavelength of 460 nm for the visualization of Hoechst 33258. The images were processed using Leica Microsystems software.

As a control, a portion that had not come into contact with the polymeric systems was subjected to the same experimental procedures and processed using the same preparation techniques.

Permeation measurements through heat-isolated porcine cheek epithelium

The HCS and TMC solutions and HCS nanoparticle suspension (100 mg) were subjected to permeation measurements by means of Franz diffusion cells (Permeager, Riegelsville, PA, USA) with a 20-mm diameter orifice (3.14 cm^2 area) thermostatted at 37 °C. Fresh porcine cheek mucosa was dipped in saline isotonic solution (pH 7.4; KH_2PO_4 1.0 g L^{-1}; Na_2HPO_4 8.10 g L^{-1};

NaCl 4.11 g L^{-1}) for 1 min at 70 °C. The epithelium was then peeled from the edges of the mucosa (Ganem-Quintanar et al 2000). The epithelium membrane was homogeneous in thickness (~750–1000 μm). A circular epithelium membrane was placed between the donor and the receptor chamber of a Franz diffusion cell. Each sample was placed on the portion of the epithelium membrane corresponding to the area of the Franz cell orifice. Then, pH 6.4 buffer (2 mL) was added over the formulation in the donor chamber to simulate the buccal environment; pH 7.4 saline isotonic solution was used as the acceptor phase. At fixed time intervals, the acceptor phase (500 μL) was withdrawn and replaced with fresh buffer. The model macromolecule FD4 was assayed by means of spectrophotometric detection using an excitation wavelength of 490 nm and an emission wavelength of 515 nm. The permeation test was also performed using 100 μL of 0.2% w/w FD4 solution, prepared in the same medium used to hydrate the polymers.

The P_{app} was calculated according to the following equation (Kotzè et al 1998):

$$P_{app} = dQ/dt\ (A \times 60 \times C_0)$$

where dQ/dt is the permeability rate (drug amount permeated per minute), A is the diffusion area of the tissue and C_0 is the initial FD4 concentration.

Statistical evaluation

Statistical differences were determined using one-way analysis of variance and post-hoc Sheffe test for multiple comparisons (Siphar software; Simed, Creteil, France). Differences between groups were considered to be significant at $P < 0.05$.

Results and Discussion

Morphological and ultrastructural findings

Light microscopy analysis

Figure 1 shows microphotographs of the sections stained with haematoxylin and eosin. The epithelial cells are stained dark, while the connective tissue corresponds to white cells (not stained with haematoxylin and eosin). The epithelial cells present dark stained nuclei and the cell plasma membranes appear as well-defined dark-stained borders. All the basal cells present nuclei and are capable of division to maintain a constant epithelial population as cells move toward the surface (tissue homeostasis requires differentiation followed by migration and desquamation of the superficial cells). The prickle cells (intermediate layer) accumulate lipids and cytokeratins and partially lose the nuclei; in the intermediate and superficial layers, nuclei are few and far between.

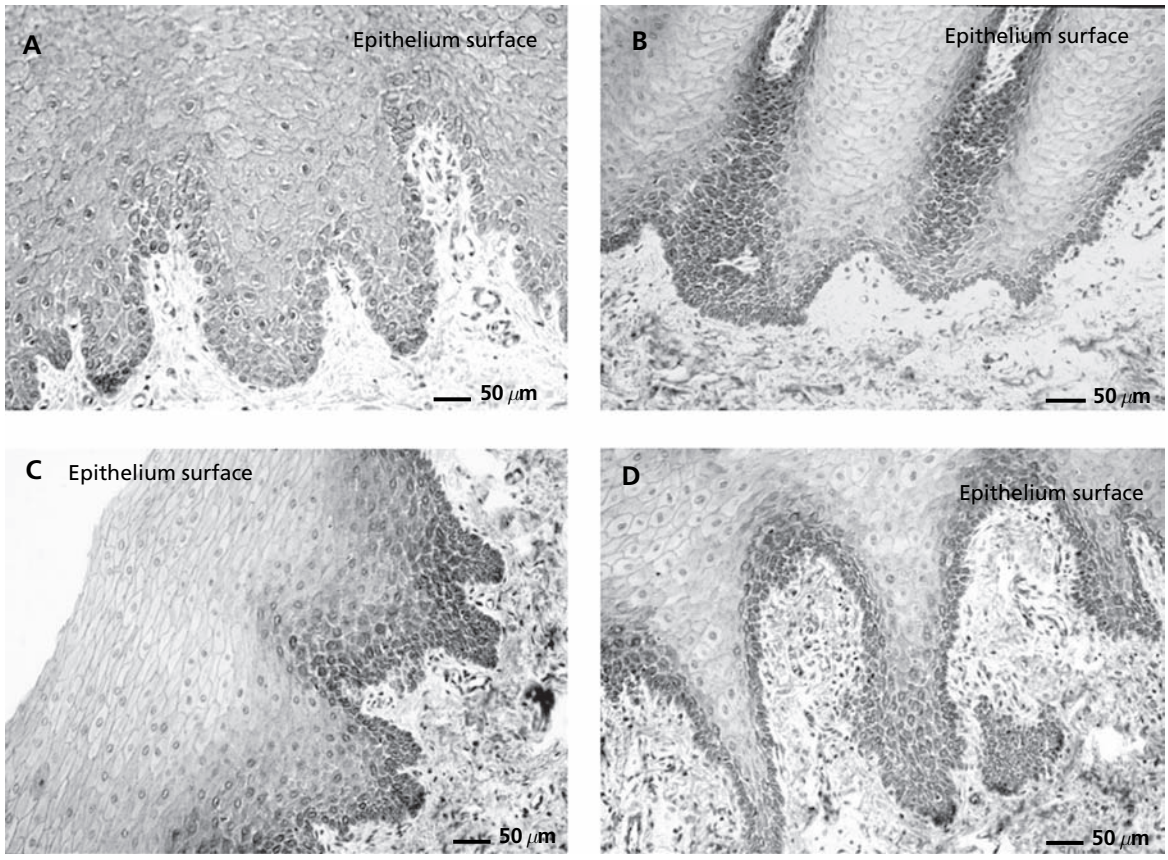

Figure 1 Microphotographs (400×) of tissue sections stained with haematoxylin and eosin: A, control; B, chitosan hydrochloride; C, trimethyl chitosan hydrochloride; D, chitosan hydrochloride nanoparticles.

In the control sample, which was not subjected to contact with polymers (Figure 1A), the basal epithelial cells are tightly bound together without any spaces between the cell plasma membranes. In particular, both the basal and the intermediate layers are characterized by viable nucleated cells (the dyes highlight the intact cell morphology) showing a cuboidal shape and smooth outlines. After treatment with HCS solution (Figure 1B), the epithelial cells of the basal and intermediate layers present a moderate constraint and large spaces between each other compared with those of the control sample (Figure 1A). After treatment with TMC solution (Figure 1C) and HCS nanoparticles (Figure 1D), the epithelial layers show the same morphological modifications observed in the tissue that had come into contact with HCS solution. Also, in these cases, the basal epithelial cells appear spaced and contracted.

The outer cell layers do not show differences in morphology between the control and the tissues that had been in contact with the polymers: no alteration was seen with respect to the control.

The morphological features described above are confirmed and easier to identify on semi-thin sections stained with Toluidine blue. Microphotographs of these samples are shown in Figure 2. The epithelial cells are stained dark while the white connective tissue cells are not stained by Toluidine blue. Toluidine blue is a basic stain used for nuclei, especially heterochromatin and nucleoli, and can indicate cell viability: cell damage causes a disorganization of the heterochromatin and the cell nuclei cannot therefore be stained. All the cells of the control were stained with blue, indicating that heterochromatin and nucleoli organization were not altered and therefore the cells were not damaged. Moreover, looking at the basal layer of the control sample (Figure 2A), all the cells appear in close contact with each other without spaces between the cell membranes (no unstained portion is visible between contiguous cells). In the inset of Figure 2A, a mitotic cell is clearly visible.

In the tissues that had been in contact with the polymer systems (Figure 2B–D), it is possible to see intercellular spaces enlarged all along the basal layer. In both the intermediate and basal cell layers, the joints between cells (with reference to desmosomes), which look like black contact points between the cells, are particularly obvious, like ridges between neighbouring cells (see arrow). This feature suggests that the cells are more spaced out than those of the control and the contact points are stretched.

In particular, in the sample of buccal mucosa that was in contact with HCS solution (Figure 2B), some cells appear swollen and show weaker staining. Furthermore, in the intermediate layers of this sample, it is possible to see a few light spots corresponding to cells not stained by Toluidine blue: the lack of staining indicates that the heterochromatin

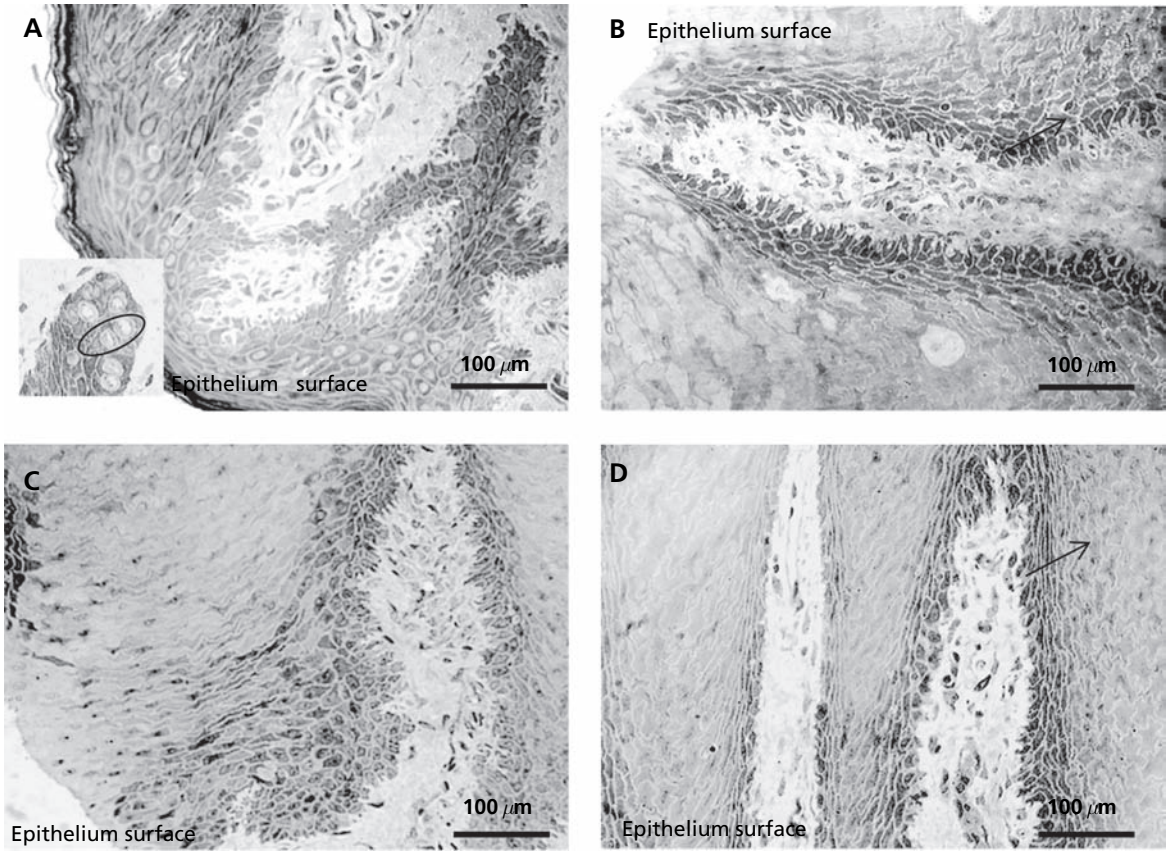

Figure 2 Microphotographs (400×) of the semi-thin sections stained with Toluidine blue: A, control (in the inset, two cells in mitosis are encircled); B, chitosan hydrochloride; C, trimethyl chitosan hydrochloride; D, chitosan hydrochloride nanoparticles.

and nucleoli are disorganized because the cells are damaged or even dead.

The epithelial mucosa samples that were in contact with TMC solution and HCS nanoparticles show a similar alteration in morphology as the tissue that had been in contact with HCS solutions (Figure 2C and D).

In the samples that were in contact with HCS and TMC solutions and with HCS nanoparticles, the cells of the intermediate layers appear swollen, suggesting drainage of water from the basal layers to the epithelium surface in direct contact with polymer systems that directly exert a water uptake effect.

Even if the cell swelling is conceivably an effect of all the polymeric systems, unstained cells can be observed only in the tissue sample that was in contact with HCS solution. This sample is probably responsible for a mild but evident damaging effect that was not evidenced in the case of the HCS nanoparticulate system or in the case of TMC solution.

Figure 3 shows the microphotographs of the semi-thin sections stained with anti-desmosomal protein antibody subjected to immunohistochemical reaction. In the control tissue (not subjected to contact with the polymers) (Figure 3A), the plasma membrane of the epithelial cells stained positive to the anti-desmosomal antibody: the plasma membranes are continuous and dense, indicating that the desmosomal proteins, constituted by transmembrane and plasma membrane associated proteins, form a close texture. The tissues that were in contact with the polymer systems (Figure 3B–D) are characterized by almost marbled plasma membrane borders. This indicates that the desmosomes in the samples subjected to exposure to HCS and TMC solution are not as well ordered and well organized as those of the control tissue: this is probably due to the enlargement of the paracellular pathways (intercellular spaces) that stretch the desmosomes and disarrange the position of the junctions.

The disarranging effect of the HCS nanoparticulate systems on intercellular junctions is in partial agreement with the literature, which reports a lack of interference of HCS nanoparticles with the junctional proteins (Fernandez-Urrursuno et al 1999), in particular with tight junctions in intestinal epithelium (Caco-2 cell monolayers) (Ma & Lim 2003).

TEM analysis

Figure 4 shows the TEM microphotographs. The epithelial cells of the control sample (Figure 4A) show a normal organization of the cell organelles: on the left side of the microphotograph of the control sample, the cell nucleus and the

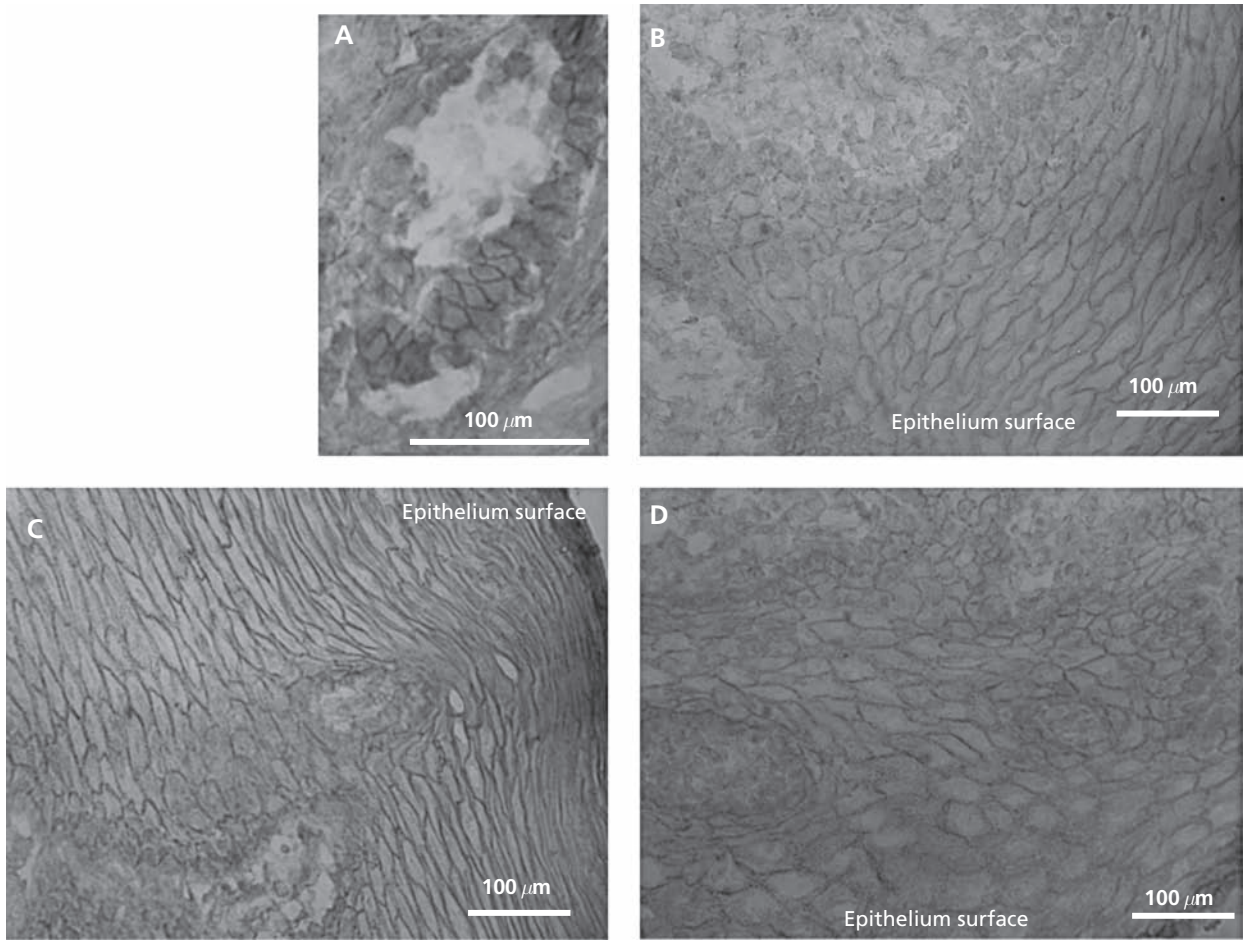

Figure 3 Microphotographs (400×) of the buccal mucosa treated with anti-desmosomal protein antibody (immunohistochemical staining): A, control; B, chitosan hydrochloride; C, trimethyl chitosan hydrochloride; D, chitosan hydrochloride nanoparticles.

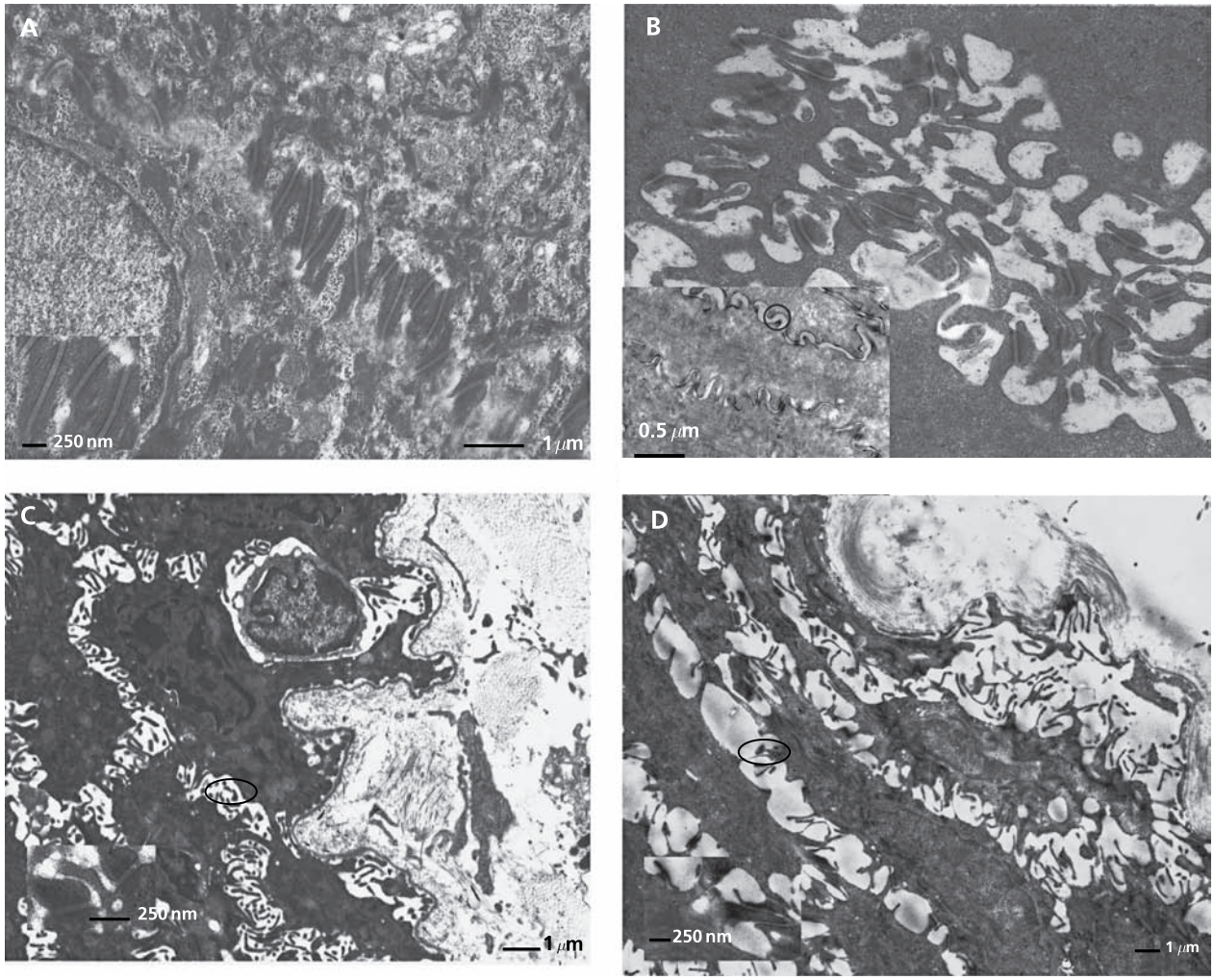

Figure 4 Transmission electron microscopy microphotographs of the buccal mucosa treated with: A, control (with a magnification of the desmosomes shown in the inset); B, chitosan hydrochloride, basal layer (with a section of the intermediate layers shown in the inset); C, trimethyl chitosan hydrochloride (with a magnification of the desmosomes shown in the inset); D, chitosan hydrochloride nanoparticles (with a magnification of the desmosomes shown in the inset).

perinuclear membrane are evident and characterized by normal morphology. The presence of bundles of intermediate filaments that radiate from the perinuclear region to the peripheral region can be seen, ending in a dense plague of numerous desmosomes. The inset to Figure 4A shows the desmosomes in detail: the protein sheets that create the desmosomal junction are visible.

Figure 4B shows that in the basal cell layer of the tissue that was in contact with HCS solution, the epithelial cells of the mucosa lose their mutual contacts: the cells are constrained and large intercellular spaces are clearly visible between the cell plasma membranes as previously reported by Senel (2002). However, the desmosomes seem stretched but not broken up. The cells of the intermediate layers (inset) are characterized by fewer intact desmosomes: the proteins that form desmosomes can still be recognized as black lines (encircled in the microphotograph) on the cell plasma membranes but they appear, in many cases, as detached due to the enlargement of the intercellular space (enlargement of the paracellular pathway). This result is in accord with the light spots observed in the semi-thin sections stained with Toluidine blue and previously identified as damaged or dead cells. Moreover, the constrained cells are characterized by wrinkled nuclei with folding perinuclear membranes. In particular, the cells lose their subcellular organization: cytoplasm lacks organelles having normal morphology.

The tissues that had come into contact with TMC solution (Figure 4C) and with HCS nanoparticles (Figure 4D) show intercellular spaces enlarged in the basal layers, even if the desmosomes in this portion of the tissue are intact and join two contiguous cells (the magnifications (insets) allow us to better appreciate that the desmosome maintains intact protein sheets in both cases). On the contrary, the junctions in the intermediate layers are disarranged and largely opened (not shown).

CLSM analysis

Figure 5 shows the CLSM microphotographs. The nuclei are light coloured on the dark black background and along the edge of the tissue surface; the FD4 permeated into the tissue beams a green signal (seen as light bands on the microphotographs).

The microphotograph of the control tissue, which did not come into contact with polymers, (Figure 5A) does not show bands of green fluorescence and only the nuclei can be observed. In the microphotographs of the tissues that were in contact with all the polymers (Figure 5B–D) it can be clearly seen that FD4 has penetrated well into the buccal tissue as the mucosa was sectioned perpendicularly to the surface. In particular, the depth of FD4 penetration into the tissues can be appreciated by looking at the bands. Both the tissues that were in contact with the two polymer solutions (HCS and TMC) are characterized by bands of variable depths along the tissue borders. In particular, the substrate in contact with HCS (Figure 5B) shows a band with a depth ranging from about 5 to 15 μm, while the substrate in contact with TMC (Figure 5C) shows a band ranging from 9.2 to 29.0 μm in depth. This suggests that TMC promotes the penetration of FD4 to a greater extent compared with HCS.

HCS nanoparticles showed a different behaviour: the band corresponding to FD4 penetration is uniform and

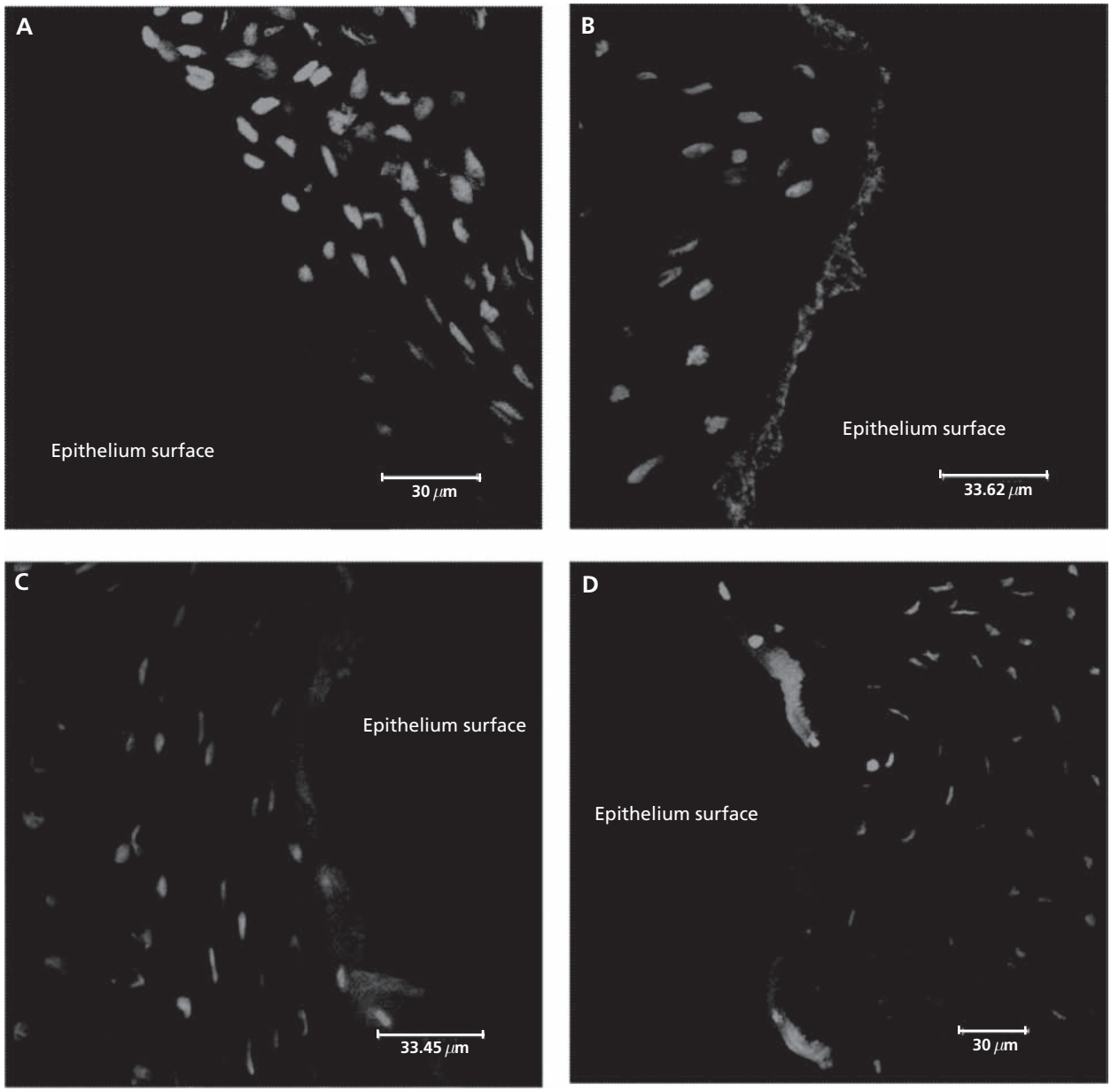

Figure 5 Confocal laser scanning microscopy microphotographs of the buccal mucosa treated with: A, control; B, chitosan hydrochloride; C, trimethyl chitosan hydrochloride; D, chitosan hydrochloride nanoparticles.

intense in colour along the tissue border. The depth of FD4 permeation ranges in this case from about 10.4 to 12.8 μm. However, it was not possible to detect spherical agglomerates of green fluorescence with reference to nanoparticles: so it is not possible to state if the nanoparticles as such go into the tissue or are only able to enhance FD4 permeation due to the widespread intensity of the green band signal.

Permeation properties through heat-isolated porcine cheek epithelium

The FD4 solution presents a very low P_{app} value ($4.3\times10^{-6}\pm8.91\times10^{-17}$ cm s^{-1}; mean ± s.e.) ($P<0.05$), indicating the poor ability of the model macromolecule FD4 to permeate through the buccal epithelium. HCS solution is characterized by an intermediate P_{app} value ($6.34\times10^{-6}\pm3.75\times10^{-7}$ cm s^{-1}; mean ± s.e.). TMC solution ($1.42\times10^{-5}\pm3.02\times10^{-6}$ cm s^{-1}; mean ± s.e.) and HCS nanoparticles ($1.40\times10^{-5}\pm2.71\times10^{-6}$ cm s^{-1}; mean ± s.e.) showed the highest P_{app} values, which were not statistically different from each other ($P<0.001$). This indicates that both the trimethylation of chitosan and chitosan in nanoparticulate form are able to improve the permeation of FD4 to a comparable extent.

Conclusions

The morphological and ultrastructural analysis performed by means of light microscopy, TEM and CLSM suggest that the mechanism of penetration enhancement of chitosan is the same for chitosan solution and the nanoparticulate form. In addition, the trimethylation of chitosan to trimethyl chitosan did not modify the mechanism of penetration enhancement.

Such a mechanism can probably be identified as a repackaging of the epithelium cells up to the basal membrane and in a partial disarrangement of desmosomes (as suggested by the TEM microphotographs). The intercellular spaces between contiguous cells were enlarged following contact with the polymers (as evidenced by means of the light microscopy and TEM). This modification could be due to the drainage of fluids from the basal layers to the intermediate and superficial layers: in the basal layers, the depletion of cell fluids could be the reason for the opening of paracellular pathways, apparently without disruption of the desmosomal structures, which were stretched but still closed. However, although the desmosomal proteins were still unaltered at cell borders, as evidenced by immunohistochemical analysis, a detachment of the junction protein sheets occurred in the intermediate layers.

It is conceivable that where the intracellular spaces are enlarged, the organized lipid lamellae that represent the major intercellular barrier in buccal epithelium are modified or even disrupted. This is in accordance with a proposed mechanism of chitosan, indicated as capable of interfering with the lipid organization in the buccal epithelium by disrupting it and causing a permeabilizing effect (Senel et al 2000). Furthermore, the penetration enhancing mechanism cannot be attributed to cell damage. Moreover, the penetration enhancement of the hydrophilic macromolecule FD4 (MW 4400 Da) indicates that both trimethyl chitosan solution and chitosan in nanoparticulate systems were able to increase FD4 permeation across buccal epithelium to a greater extent than chitosan solution. The permeation enhancement together with the well-established mucoadhesive properties of chitosan and trimethyl chitosan make trimethyl chitosan and chitosan nanoparticles promising candidates for the development of buccal formulations aiming to improve the systemic bioavailability of hydrophilic, high molecular weight molecules such as poorly absorbable peptide drugs.

References

Artursson, P., Lindmark, T., Davis, S. S., Illum, L. (1994) Effect of chitosan on the permeability of monolayers of intestinal epithelial cells (Caco-2). *Pharm. Res.* **11**: 1358–1361

Behrens, I., Vila-Pena, A. I., Alonso, M. -J., Kissel, T. (2002) Comparative uptake studies of bioadhesive and non-bioadhesive nanoparticles in human intestinal cell lines and rats: the effect of mucus on particle absorption and transport. *Pharm. Res.* **19**: 1185–1193

Calvo, P., Remunan-Lopez, C., Vila-Jato, J. L., Alonso, M. J. (1997) Novel hydrophilic chitosan-polyethylene oxide nanoparticles as protein carriers. *J. Appl. Polym. Sci.* **63**: 125–132

Di Colo, G., Burgalassi, S., Zambito, Y., Monti, D., Chetoni, P. (2004) Effects of different N-trimethyl chitosans on in vitro/in vivo ofloxacin transcorneal permeation. *J. Pharm. Sci.* **93**: 2851–2862

Dodane, V., Amin Khan, A., Mervin, J. R. (1999) Effect of chitosan on epithelial permeability and structure. *Int. J. Pharm.* **182**: 21–32

Fernandez-Urrursuno, R., Calvo, P., Remunan-Lopez, C., Vila-Jato, J. L., Alonso, M. J. (1999) Enhancement of nasal absorption of insulin using chitosan nanoparticles. *Pharm. Res.* **16**: 1576–1581

Ganem-Quintanar, A., Guintanar-Guerrero, D., Buri, P., Jacques Y. (2000) Permeability of phentanyl solutions and lipids composition of buccal epithelium surgically isolated versus heat-separated. Proceedings of the 27th Annual Meeting of the Controlled Release Society

Hamman, J. H., Stander, M., Kotzè, A. F. (2002) Effect of the degree of quaternization of N-trimethyl chitosan chloride on absorption enhancement: in vivo evaluation in rat nasal epithelia. *Int. J. Pharm.* **232**: 235–242

Hamman, J. H., Schultz, C. M., Kotzè, A. F. (2003) N-Trimethyl chitosan chloride: optimum degree of quaternization for drug absorption enhancement across epithelial cells. *Drug Dev. Ind. Pharm.* **29**: 161–172

Kotzè, A. F., Lueβen, H. L., de Leeuw, B. J., de Boer, A. G., Verhoef, J. C., Junginger, H. E. (1998) Comparison of the effect of different chitosan salts and N-trimethyl chitosan chloride on permeability of intestinal epithelial cells (Caco-2). *J. Control. Release* **5**: 35–46

Ma, Z., Lim, L.-Y. (2003) Uptake of chitosan associated insulin in Caco-2 cell monolayers: a comparison between chitosan molecules and chitosan nanoparticles. *Pharm. Res.* **20**: 1812–1819

Paul, W., Sharma, C. P. (2000) Chitosan, a drug carrier for 21st century: a review. *STP Pharma. Sci.* **10**: 5–22

Reichl, S., Muller-Goymann, C. C. (2003) The use of a porcine organotypic cornea construct for permeation studies from formulations containing befunolol hydrochloride. *Int. J. Pharm.* **250**: 191–201

Rossi, S., Sandri, G., Ferrari, F., Bonferoni, M. C., Caramella, C. (2003a) Buccal delivery of acyclovir from films based on chitosan and polyacrylic acid. *Drug Dev. Ind. Pharm.* **8**: 199–203

Rossi, S., Sandri, G., Ferrari, F., Bonferoni, M. C., Caramella, C. (2003b) Development of films and matrices based on chitosan and polyacrylic acid for vaginal delivery of acyclovir. *STP Pharma. Sci.* **13**: 183–190

Rossi, S., Sandri, G., Caramella, C. (2005) Buccal drug delivery: a challenge already won? *Drug Discov. Today: Technologies* **2**: 59–65

Sandri, G., Rossi, S., Ferrari, F., Bonferoni, M. C., Muzzarelli, C., Caramella, C. (2004) Assessment of chitosan derivatives as buccal and vaginal penetration enhancers. *Eur. J. Pharm. Sci*. **21**: 351–359

Sandri, G., Bonferoni, M. C., Rossi, S., Ferrari, F., Zambito, Y., Di Colo, G., Caramella, C. (2005a) Nanoparticles based on trimethylchitosans: influence of the degree of quaternization. 32th Annual Meeting of the Controlled Release Society

Sandri, G., Rossi, S., Bonferoni, M. C., Ferrari, F., Zambito, Y., Di Colo, G., Caramella, C. (2005b) Buccal penetration enhancement properties of N-trimethyl chitosan: influence of quaternization degree on absorption of a high molecular weight molecule. *Int. J. Pharm*. **297**: 146–155

Sayani, A. P., Chien, Y. W. (1996) Systemic delivery of peptides and proteins across absorptive mucosae. *Crit. Rev. Ther. Drug Carrier Syst*. **13**: 85–184

Senel, S., Hincal, A. A. (2001) Drug permeation enhancement via buccal route: possibilities and limitations. *J. Control. Release* **72**: 133–144

Senel, S., Kremer, M. J., Kas, S., Wertz, P. W., Hincal, A. A., Squier, C. A. (2000) Enhancing effect of chitosan on peptide drug delivery across buccal mucosa. *Biomaterials* **21**: 2067–2071

Senel, S., Kremer, M. J., Wertz, Hill J. R., Kas, S., P. W., Hincal, A. A., Squier, C. A. (2002) Chitosan for intraoral peptide delivery. In: Muzzarelli, R. A. A., Muzzarelli, C. (eds) *Chitosan in pharmacy and chemistry*. ATEC, Italy, pp 77–84

Shojaei, A. H. (1998) Buccal mucosa as a route for systemic drug delivery: a review. *J. Pharm. Sci.* **1**: 15–30

Sieval, A. B., Thanou, M., Kotzè, A. F., Verhoef, J. C., Brussee, J., Junginger, H. E. (1998) Preparation and NMR characterization of highly substituted N-trimethyl chitosan chloride. *Carbohydr. Res*. **36**: 175–165

Thanou, M. M., Kotze, A. F., Scharringhausen, T., Lueβen, H. L., de Boer, A. G., Verhoef, J. C., Junginger, H. E. (2000) Effect of degree of quaternization of N-trimethyl chitosan chloride for enhanced transport of hydrophilic compounds across intestinal Caco-2 cell monolayers, *J. Control. Release* **64**: 15–25

Yi, X., Wang, Y., Yu, F. S. (2000) Corneal epithelial tight junctions and their response to lipopolysaccharide challenge. *Invest. Ophthalmol. Vis. Sci*. **41**: 4093–4100